Note

Ceres – Neither a porous nor salty ball

Julie C. Castillo-Rogez

Jet Propulsion Laboratory, California Institute of Technology, Pasadena, CA 91109, USA

ARTICLE INFO

ABSTRACT

This study explores the geophysical implications of two compositional models recently proposed for Ceres, which assume that the dwarf planet is a homogeneous mixture of chondritic material devoid with free water. In order to reproduce Ceres' density, the rock density has to be offset by the presence of porosity and/or an abundance of hydrated salts resulting from the extensive hydration and oxidation of the chondritic material. Thermal modeling shows that a mixture of hydrated minerals is bound to compact and partly dehydrate as a consequence of long-lived radioisotope decay heat. The resulting interior structure is differentiated in a silicate-rich core and water-rich shell, with little porosity. Hence, this study confirms previous suggestion that Ceres contains a large fraction of free water.

© 2011 Elsevier Inc. All rights reserved.

1. Introduction

The nature of water in C-class asteroids is a long-standing question that bears important implications for assessing the astrobiological significance of these objects. The present study addresses the question of the state of water in the dwarf planet Ceres, as the current state-of-the-art opposes two very different views of its interior: the "icy" model assumes that Ceres can be compared to a "warm icy satellite" with an icy shell and rocky core (McCord and Sotin, 2005; Castillo-Rogez and McCord, 2010), while the "rocky model" assumes that water is bounded to minerals in the form of hydrated salts and silicates (Zolotov, 2009 – hereafter referred to as Z09). These two models entail very different framework for formulating science questions that will drive the science planning of the *Dawn* mission, which will reach Ceres in 2015. Comparison between these models, for example in terms of geological setting, is limited by the absence of geophysical modeling for the rocky model. Indeed, the interior structure proposed by Z09 is a static chemical model meant to explain Ceres' current state, but its geodynamical evolution remains to be investigated. This is the focus of the present study.

The recent detections of water ice and organics at the surface of the largest member of the Themis family, 24 Themis (e.g., Rivkin and Emery, 2010) and of 65 Cybele (Licandro et al., 2011) are important clues for this problem. 24 Themis appears to be the remnant core of a larger water-rich asteroid (Castillo-Rogez and Schmidt, 2010), indicating that at least in some of the large, wet asteroids, water must be buried below a thick regolith layer, as suggested by, e.g., Fanale and Salvail (1989). The simplest explanation for the absence of ice at the surface of Ceres is that water is not stable in that region of the Solar System – ~2.7 AU from the Sun versus ~3.1 AU for Themis (e.g., Schörghofer, 2008). Alternatively, the gradient in hydrated mineral abundance across the asteroid belt has been interpreted as increased thermal processing closer to the Sun due to variations in the timing of formation, which determines the amount of short-lived radioisotopes accreted into the objects (Ghosh et al., 2006). It has also been suggested that icy planetesimals were extensively processed prior to accretion, leading to aqueous alteration of the rocky material and water loss (Wilson et al., 1999). The "rocky" model may have been formed from such planetesimals, after ^{26}Al was mostly extinct (Z09). This requires a late formation timeframe with respect to that generally envisioned for Ceres-size asteroids (e.g., Weidenschilling, 2008), but this may be acceptable in absence of definitive constraints on the early Solar System history.

In order to assess the viability of the "rocky" interior scenario, I investigate its evolution over Ceres' lifetime. Especially, I test the assertion made in Z09 that "*After the accretion (after 7–8 Ma after the formation CAIs), limited heat sources* (McCord and Sotin, 2005) *could have not caused mineral dehydration and major density stratification.*" This claim is unsupported by both McCord and Sotin (2005) and Castillo-Rogez and McCord (2010). Both studies agree that Ceres' core could reach a temperature of 400 K in a few hundred Myr after accretion, at which time many hydrated materials and organics start melting and separate from the silicate phase (Kargel, 1991). I tailor a geophysical model using the same conditions as assumed by Z09 in terms of time of formation time and chemistry (Section 2). The results of this investigation are discussed in Section 3.

2. Geophysical evolution

Zolotov (2009) introduced two variants of the same idea, as a function of the degree of oxidation of planetesimal material. One model assumes that CI chondrites are good analogs for Ceres' material and requires at least 10% bulk porosity to account for the observed density (Table 1). CI material is a mixture of serpentines, tochilinite, montmorillonite, magnetite, gypsum, organics, epsomite, bloedite, and a number of minor species. I choose a content in hydrated salts based after Kargel (1991) who studied in detail the fate of these species in large chondritic bodies. Our model also includes 7 vol.% magnetite (after Nagy et al., 1963), 8 vol.% organics (Pearson et al., 2006), the rest being dominated by antigorite (the serpentine mineral most stable at Ceres' pressures), and montmorillonite (Table 1).

The other model assumes extensive oxidation of carbonaceous chondrite material in planetesimals leading to a significant volume fraction of hydrated salts (Table 2). The latter model, detailed in Table 3 of Z09, is an assemblage of hydrated silicates (37 vol.%), hydrated salts (36 vol.%), oxides (14 vol.%), and organics (6 vol.%). Its mean density is ~2.24 g/cm³. Z09 quotes 1.9 g/cm³, but this does not appear consistent with the content of his Table 3. We refer to these models as the high- and low-grain density endmembers, respectively. Both models assume accretion after short-lived radioisotopes are mostly decayed and bear little geophysical significance. I also assume no heating converted from accretional energy. Thus, the main heat source driving geophysical evolution in this framework comes from long-lived radioisotope decay.

2.1. Initial interior structures

The chemical models introduced in Z09 are representative of the initial states of the geophysical models I aim to develop. The low-density endmember does not

E-mail address: Julie.C.Castillo@jpl.nasa.gov

Table 1

Mineralogical composition of the high-density model considered in this study and physical properties relevant to this study. Minerals representing less than 1 vol.% are not included in the discussion, because they have little affect on the mechanical or thermal behavior of the mixture (Ni-sulfide, dolomite, quartz, Ca-phosphate, hydrohalite, and minor phases). The average density for that mixture is ~2.46 g/cm³, consistently with average carbonaceous chondrite material (Britt et al., 2002). Pyrene is used as a proxy to represent the organic material, following Z09's approach. Thermal data are from Prieto-Ballesteros and Kargel (2005) (epsomite and mirabilite), and Akbulut et al. (2006) (pyrene). The thermal conductivity of magnetite is expressed as a function of temperature *T* (Molgaard and Smeltzer, 1971). Specific heat data for serpentine, montmorillonite, magnetite, and halite are from Waples and Waples (2004). Full dehydration of epsomite proceeds in several steps, starting at 298 K and completing at 548 K (Van Essen et al., 2009). The most significant step occurs at a temperature of about 353 K. For the sake of simplicity, we have assumed in the modeling a one-step dehydration event at the latter temperature.

Mineral	Volume fraction	Density (g/cm³)	Dehydration (D) or melting (M) temperature (K)	Thermal conductivity (W/m/K)	Specific heat capacity (J/kg/K)
Serpentine	0.45	2.52 (average)	775 (D)	$(0.404 + 0.000246T)^{-1}$	~2000
Montmorillonite	0.15	2.32	1073 (D)	0.75	900
Magnetite	0.07	5.175	N/A	$4.23 - 1.37 \times 10^{-3}T$	586
Epsomite	0.1	1.68	353 (D)	~0.4	1546
Mirabilite	0.07	1.57	305 (D)	~0.6	1825
Pyrene	0.06	1.27	~420 (M)	~0.27	1300
Halite	0.05	~2.07	1074 (M)	5.78–1.5 f(T)	926

Table 2

Same as Table 1 but for the low-density endmember model (see text for details), based after Zolotov (2009), Table 3. The average density for that mixture is 2.24 g/cm³. Gypsum starts dehydrating at 373 K with the production of a hemihydrate, and then the production of anhydrite at 423 K (Brantut et al., 2011). Mirabilite is considered, instead of bloedite, due to the lack of thermophysical data on the latter. Thermal data are from Clauser and Huenges (1995) (gypsum), Molgaard and Smeltzer (1971) (hematite).

Mineral	Volume fraction	Density (g/cm³)	Dehydration (D) or melting (M) temperature (K)	Thermal conductivity (W/m/K)	Specific heat capacity (J/kg/K)
Saponite	0.37	2.32	1073 (D)	0.75	900
Epsomite	0.29	1.68	353 (D)	~0.4	1546
Hematite	0.14	5.3	>1800 (M)	$8.39 - 6.63 \times 10^{-3}T$	620
Mirabilite	0.07	1.57	305 (D)	~0.6	1825
Pyrene	0.06	1.27	~420 (M)	~0.27	1300
Gypsum	0.03	2.36	373–423 (D)	~0.15	1090–1800

require any porosity to explain the observed density, between 2.07 and 2.24 g/cm³, depending on available measurements (Thomas et al., 2005; Carry et al., 2008). On the other hand, the high-density endmember requires at least 10% of silicate in bulk to offset the density of CI-like material, in order to match the observed density. Zolotov (2009) suggested that the preservation of porosity down to Ceres' core, i.e., a pressure of ~150 MPa, is supported by the experimental literature, taking sandstones as an analog. Although I adopt the porosity profile presented in that study, I do not necessarily endorse it, because the compressive strengths of hydrated materials are generally lower than those characteristic of sandstones. The compressive strength of chondritic material appears to be of the order of 10 MPa (Grimm and McSween, 1989), instead of the value of 60 MPa used by Z09.[1] This means that extensive compaction of the interior (porosity ⩽10%) could be reached 20 km below the surface, instead of the ~120 km considered in Z09.

2.2. Thermal properties

Most of the minerals listed in Tables 1 and 2 have a thermal conductivity less than 1 W/m/K, and possibly as low as 0.1 W/m/K. The thermal conductivity of a solid mixture is computed as a linear combination of the minerals conductivities and volume fractions. In the case of the low-density endmember, the thermal conductivity is of the order of 1.4 W/m/K at 200 K and decreases to 1 W/m/K at 700 K, mainly due to the strong dependence of hematite on temperature.

In the case of the high-density endmember, the presence of porosity makes it more difficult to estimate thermal conductivity. Its impact is a function of the void geometry, which determines the number of contacts between grains. The assemblage of various compounds, some of which may act as cement between grains or fill in veins within the material, makes the problem even more difficult to constrain. The thermal conductivity of the solid endmember composition is about 2.4 W/m/K at 200 K. However, if the porosity is significant, it becomes the main factor determining thermal conductivity (e.g., Shoshany et al., 2002). As a reference, a CM chondrite sample with a porosity of ~37% has a bulk thermal conductivity of 0.5 W/m/K, with little dependence on temperature (Opeil et al., 2010). Also, the thermal conductivity of martian regolith analog with a porosity of ~50% is of the order of 0.1 W/m/K at a temperature of 200 K (Zent et al., 2010) similar to Ceres' subsolar temperature (Fanale and Salvail, 1989). I use the latter value in the modeling, keeping in mind that that parameter may be even further reduced in Ceres' outermost material (Jeff Kargel, personal communication).

---

[1] Compressive strength is the maximum stress a material can undergo until failure. It determines compaction as a consequence of brittle deformation (as a difference to creep-driven porosity collapse).

The mean specific heat capacities of the mixtures can be computed as a linear combination of the capacities of each mineral and their mass fractions. Specifics for each models are indicated in Fig. 1.

2.3. Thermal evolution

As a first-order approximation, I compute the thermal evolution of a spherical body subject to long-lived radioactive decay heat (e.g., McCord and Sotin, 2005; Castillo-Rogez et al., 2007): Heat transfer is computed after:

$$\frac{\partial \left(k(T) \cdot \frac{\partial T(r)}{dr} \right)}{\partial r} + \frac{2}{r}\left(k(T)\frac{\partial T(r)}{\partial r} \right) = \rho(r)C_p(T)\left(\frac{dT(r)}{dt} \right) - H(r) \tag{1}$$

where *T* is temperature, *r* is the local radius, *k* is the thermal conductivity, ρ is the material density, C_p is the specific heat capacity, *t* is time, and *H* represents the internal heating. Internal evolution is marked by two major processes: the dehydration and/or melting of most minerals involved in the two endmember models and the compaction of the silicate compounds. By thermogravimetry analysis, Nagy et al. (1963) tracked the loss of 22% of material mass from CI chondrite gradually heated from 373 to 1273 K, with major steps between 373 and 473 K, 773–873 K and 1050–1200 K. These may be attributed to the dehydration of salt hydrates, serpentine (antigorite), and montmorillonite, respectively (Nagy et al., 1963; Tables 1 and 2). Accounting for the melting of these compounds is a major improvement upon the modeling approach previously used by Castillo-Rogez and McCord (2010). Indeed, part of radioisotope decay heating is used as latent heat for these multiple reactions. Hence these events delay the time at which silicate dehydration occurs. The latent heat for gypsum is 98 kJ/kg (Brantut et al., 2011), 932 kJ/kg for epsomite (Van Essen et al., 2009), and 131 kJ/mol for clay. Montmorillonite and serpentines dehydrate at higher temperatures.

The creep of antigorite, the serpentine endmember relevant to Ceres' relatively high pressures, is activated with an energy as low as a few tens kJ/mol (Hilairet et al., 2007). These authors found a relaxation time shorter than ~10^4 years at a temperature of 473 K, for a differential stress greater than 1 MPa, which is relevant to our study. Measurements of serpentine creep properties are scarce though, and the weakness of antigorite is currently a matter of debate. Still, even if the relaxation times obtained by Hilairet et al. (2007) results were off by several orders of magnitude, silicate relaxation would still be warranted since Ceres' interior was likely to bear temperatures greater than 473 K for most of its history (Fig. 1).

The temperature achieved in the interior model as a function of time and radius is displayed in Fig. 1. For both models, part of Ceres volume starts melting about 200 Myr after formation. Melting and separation of the hydrated salts, pyrene, and water from gypsum occur over a timescale of about 200 Myr determined in part by the large latent heat of epsomite. This event affects about 23 vol.% of the
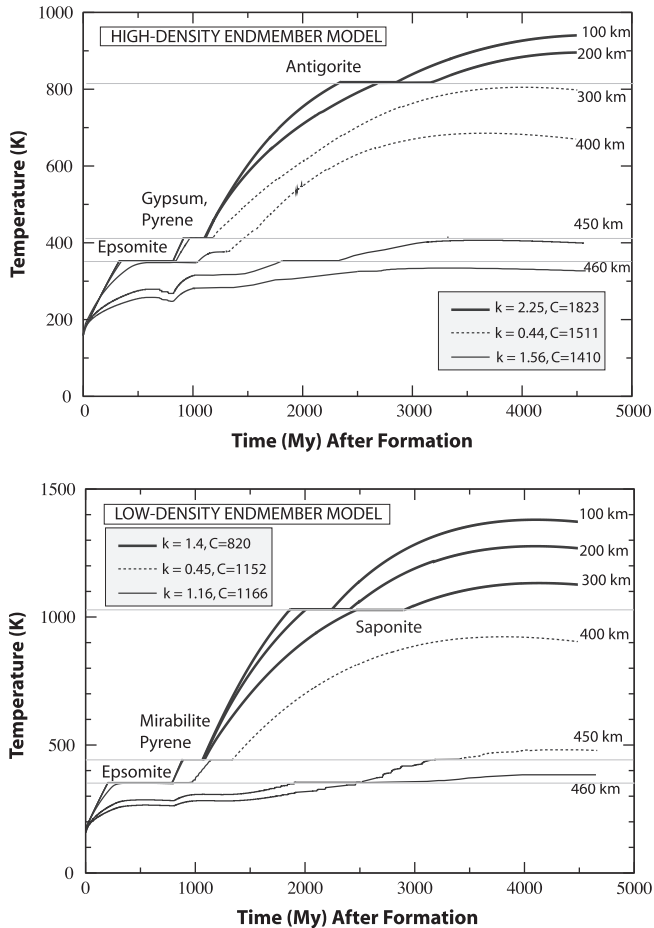
Fig. 1. Maximum temperature achieved in Ceres' interior models as a function of radius (100, 200, 300, 400, 450, 460 km) for the two compositions considered in this study. (Bottom) Low-density, oxidized endmember. (Top) High-density, CI-chondrite endmember. These models assume no initial heating from accretional energy. The evolution is marked by a major reorganization when the temperature reaches 350–450 K, at which many of the minerals start melting and separate from a phyllosilicate-enriched core. The parameters k and C indicate the average values of the thermal conductivity (W/m/K) and specific heat capacity (J/kg/K), respectively, as a function of depth and main stages of the evolution.

high-density endmember model and 45 vol.% of the low-density model. This results in a major change in the structure of the object. Low-density solutions separate from the denser phyllosilicates. In the high-density, porous endmember, deep porosity within the silicate is filled in with brines. At a later stage, about 600 Myr after formation, serpentine starts compacting and that process may extend over 10^4 years to several hundred Myr, until completion. The prospect for the rocky core to achieve the dehydration temperature of antigorite or saponite is a function of the long-term evolution of the overlaying shell, as that layer controls the rate at which heat is removed from the core. This is discussed in detail below.

2.4. Final interior structures

The melting and separation of hydrated species from chondritic material upon heating was explored in depth by Kargel (1991). Dehydration is generally accompanied by changes in permeability (e.g., Hoogerduijn Stratinga and Vissersa, 1991), creating a path for solutions to percolate toward the surface. Hydrated salts, organics, and water can recondense as a function of temperature and specific gravity (Kargel, 1991, e.g., Fig. 9a). Kargel (1991) showed that the fractionated crystallization of brines leads to the separation of about 5 vol.% of free water in the shell. This study also confirms Kargel's suggestion that in large chondritic cores, gypsum should dehydrate as well, thus leading to further enrichment of the shell in free water.

Such a stratified shell is likely to be stable against convection, in which case the temperature achieved in these poorly conductive layers can be significant and lead to a second stage of melting, and may be expressed in the form of cryovolcanism (Kargel, 1991; Prieto-Ballesteros and Kargel, 2005). Detailed mod-

eling of the thermal evolution of that shell is a complex problem beyond the scope of the present study. Since the evolution of the shell controls the history of heat removal from the core, I cannot determine whether deep phyllosilicates can achieve a temperature greater than 800 K, at which they start dehydrating, resulting in further migration of water from the core to an outer icy shell. In the warmest possible case, up to 10% of antigorite may dehydrate, starting about 1 Gyr after formation. Dehydration of saponite occurs at a later stage in the low-density endmember model, but may still affect about 20% of the volume of that mineral (Fig. 1a and b). In the case of the high-density endmember model, the dehydration temperature for epsomite is reached about 15 km below the surface. Dehydration temperatures for gypsum and pyrene are achieved ~25 km deep. In the case of the low-density endmember model, dehydration of epsomite is even more extensive due to the insulating role of the very porous outer layer, and affects almost 95% of the interior model volume (i.e., up to a depth of about 7 km). In summary, only the outermost 10–20 km of the dwarf planet model remains at temperatures cool enough for the original composition to be preserved. While a surface porosity greater than 40% has been inferred from Arecibo and Goldstone Radar observations (Mitchell et al., 1996), the material is expected to undergo creep at shallow depths, accommodated in particular by the viscous flow of organics and hydrates at low temperature. It is also likely that that outer layer would overturn, for example if it is disturbed by stress resulting from volume changes and impacts.

As a consequence of compaction, the high-density endmember achieves a density of ~2.46 g/cm³, which is inconsistent with observations. Indeed that model is intrinsically deficient in water (the water mass fraction x_w is ~27% in the ice–rock mixture (McCord et al., 2011, Fig. 1), while x_w is only ~17% in the present case.

Macroporosity developed in the outer shell posterior to the main evolution events may reduce the density somewhat but not to the extent needed to explain the observed density. The *entire* outer shell would have to hold a macroporosity of at least 50% in order to adequately offset the grain density. A volatile-rich shell is likely to relax at the warm surface temperature of Ceres and is unlikely to preserve macroporosity below 10 km, i.e., at pressures greater than 1 MPa. Indeed, at a temperature of 180 K the relaxation time of a water-ice rich material is of the order of thousand years (see Castillo-Rogez et al. (2011) for ice relaxation time calculation). The fact that Ceres' shape appears in hydrostatic equilibrium and the absence of large (⩾60 km diameter) craters at the surface of the asteroid (Thomas et al., 2005) also suggest that its outer material can easily relax on geological timescales in contrast to, e.g., Pallas (Schmidt et al., 2009).

On the other hand, the low-density endmember allows for almost as much water (~22%) as in the ice-rich model, stored in the form of water of hydration in epsomite, in particular. Hence, even after partial melting of the interior, the final structure is characterized by a density of ~2.24 g/cm³, which is within the range of density inferred by Z09 from the Carry et al. (2008) shape determination. It is about 10% greater than the density value inferred by Thomas et al. (2005) though. Refined shape and mass data from the *Dawn* Mission will resolve that uncertainty.

3. Conclusions

I showed that the long-term evolution of the rocky models introduced by Z09 is determined by the low creep and melting temperatures of some of the hydrated phases and organics. This leads to rapid compaction of the interior and chemical differentiation accompanied by the segregation of a fraction of "free" water. The end-result model is layered with a rocky core and an outer shell enriched in hydrated salts, organics, and water ice, a structure similar to that proposed by Castillo-Rogez and McCord (2010) starting with different initial conditions. Further modeling of the shell is necessary in order to understand the long-term evolution of the core in this context and quantify the total amount of water released from the silicates.

Since the high-density endmember model was developed under the assumption that Ceres could sustain some porosity over the long term, the thermal model presented here invalidates such a model. Devoid with porosity, its density is now at least 10% greater than the upper bound on the observed value. While the low-density chemical model remains consistent with Ceres' density (upper bound), one must keep in mind that it relies on extreme assumptions on the oxidization state of the material accreted in the dwarf planet. The viability of such a scenario and its consistency with available constraints on Ceres' chemistry, i.e., detection of brucite and carbonates (Milliken and Rivkin, 2009) remain to be tested.

This study does not question the possibility that smaller C-class asteroids may be made up of porous carbonaceous chondrite material though. It simply points out that such an assemblage is likely to be unstable in an object of Ceres' size, which could achieve moderate to high temperatures in the course of its evolution. A model in which water is partly in the form of ice appears most consistent with the dwarf planet's properties, which puts Ceres in the same class as the Themis parent body (Castillo-Rogez and Schmidt, 2010).

More generally, this work is also relevant to other studies that have suggested a chondritic composition for the cores of large icy satellites (e.g., Fortes, 2011, for Titan). The destabilization of a large fraction of the hydrated material is warranted

at the temperatures expected in these large cores, with potentially significant thermal and mechanical consequences.

Acknowledgments

References

Akbulut, S., Ocak, Y., Böyük, U., Erol, M., Keşlioğlu, K., Maraşli, N., 2006. Measurement of solid–liquid interfacial energy in the pyrene succinonitrile monotectic system. J. Phys.: Condens. Matter 18, 8403–8410.

Brantut, N., Han, R., Shimamoto, T., Findling, N., Schubnel, A., 2011. Fast slip with inhibited temperature rise due to mineral dehydration: evidence from experiments on gypsum. Geology 39 (1), 5962. doi:10.1130/G31424.1.

Britt, D.T., Yeomans, D., Housen, K., Consolmagno, G., 2002. Asteroid density, porosity, and structure. In: Bottke, W.F., Jr. et al. (Eds.), Asteroids III. Univ. of Arizona, Tucson.

Carry, B. et al., 2008. Near-infrared mapping and physical properties of the dwarf-planet Ceres. Astron. Astrophys. 478, 235–244.

Castillo-Rogez, J., Matson, D.L., Sotin, C., Johnson, T.V., Lunine, J.I., Thomas, P.C., 2007. Iapetus geophysics: Rotation rate, shape, and equatorial ridge. Icarus. doi:10.1016/j.icarus.2007.02.018.

Castillo-Rogez, J.C., Schmidt, B., 2010. Geophysical evolution of the Themis family parent body. Geophys. Rev. Lett. 37, L10202.

Castillo-Rogez, J.C., McCord, T.B., 2010. Ceres evolution and present state constrained by shape data. Icarus 205, 443–459. doi:10.1016/j.icarus.2009.04.008.

Castillo-Rogez, J.C., Efroimsky, M., Lainey, V., 2011. The tidal history of Iapetus. Spin dynamics in the light of a rened dissipation model. J. Geophys. Res., 116, in press. doi:10.1029/2010JE003664.

Clauser, C., Huenges, E., 1995. Thermal conductivity of rocks and minerals. In: Ahrens, T.J. (Ed.), Rock Physics and Phase Relations: A Handbook of Physical Constants, vol. 3. AGU Reference Shelf, American Geophysical Union, WA, pp. 105–126.

Fanale, F., Salvail, J.R., 1989. The water regime of Asteroid (1) Ceres. Icarus 82, 97–110. doi:10.1016/0019-1035(89)90026-2.

Fortes, A.D., 2011. Titans internal structure and the evolutionary consequences. Icarus. doi:10.1016/j.pss.2011.04.010.

Ghosh, A., Weidenschilling, S.J., McSween Jr., H.Y., Rubin, A., 2006. Asteroidal heating and thermal stratification of the asteroid belt. In: Lauretta, D., McSween, H.Y. (Eds.), Meteorites and the Early Solar Systems II, vol. 942. University of Arizona Press, pp. 555–566.

Grimm, R.E., McSween Jr., H.Y., 1989. Water and the thermal evolution of carbonaceous chondrite parent bodies. Icarus 82, 244280.

Hilairet, N. et al., 2007. High-pressure creep of serpentine, interseismic deformation, and initiation of subduction. Science 318, 1910–1912. doi:10.1126/science.1148494.

Hoogerduijn Stratinga, E.H., Vissersa, R.L.M., 1991. Dehydration-induced fracturing of eclogite-facies peridotites: Implications for the mechanical behaviour of subducting oceanic lithosphere. Tectonophysics 200, 187–198. doi:10.1016/0040-1951(91)90014-J.

Kargel, J.S., 1991. Brine volcanism and the interior structures of asteroids and icy satellites. Icarus 94, 368–390.

Licandro, J. et al., 2011. (65) Cybele: Detection of small silicate grains, water-ice, and organics. Astron. Astrophys. 525, A34. doi:10.1051/0004-6361/201015339.

McCord, T.B., Sotin, C., 2005. Ceres: Evolution and current state. J. Geophys. Res. 110, CiteID E05009.

McCord, T.B., Casitllo-Rogez, J.C., Rivkin, A.S., 2011. Ceres: Its origin, evolution and structure and dawns potential contribution. Space Sci. Rev.. doi:10.1007/s11214-010-9729-9.

Milliken, R.E., Rivkin, A., 2009. Brucite and carbonate assemblages from altered olivine-rich materials on Ceres. Nat. Geosci. 2, 258–261. doi:10.1038/NGEO478.

Mitchell, D.L., Ostro, S.J., Hudson, R.S., Rosema, K.D., Campbell, D.B., Velez, R., Chandler, J.F., Shapiro, I.I., Giorgini, J.D., Yeomans, D.K., 1996. Radar observations of Asteroids 1 Ceres, 2 Pallas, and 4 Vesta. Icarus 124, 113–133. doi:10.1006/icar.1996.0193.

Molgaard, J., Smeltzer, W.W., 1971. Thermal conductivity of magnetite and hematite. J. Appl. Phys. 42, 3644–3647.

Nagy, B., Meinschein, W.G., Hennessy, D.J., 1963. Aqueous, low temperature environment of the Orgueil meteorite parent body. Ann. NY Acad. Sci. 108, 534–552.

Opeil, C.P., Consolmagno, G.J., Britt, D.T., 2010. The thermal conductivity of meteorites: New measurements and analysis. Icarus 208, 449–454.

Pearson, V.K., Sephton, M.A., Franchi, I.A., Gibson, J.M., Gilmour, I., 2006. Carbon and nitrogen in carbonaceous chondrites: Elemental abundances and stable isotopic compositions. Meteorit. Planet. Sci. 41, 1899–1918.

Prieto-Ballesteros, O., Kargel, J.S., 2005. Thermal state and complex geology of a heterogeneous salty crust of Jupiter's satellite, Europa. Icarus 173, 212–221.

Rivkin, A.S., Emery, J.P., 2010. Detection of ice and organics on an asteroidal surface. Nature 464, 1322–1323. doi:10.1038/nature09028.

Schmidt, B.E. et al., 2009. The shape and surface variation of 2 Pallas from the Hubble Space Telescope. Science 326, 275–279. doi:10.1126/science.1177734.

Schörghofer, N., 2008. The lifetime of ice on main belt asteroids. Astrophys. J. 682, 697–705.

Shoshany, Y., Prialnik, D., Podolak, M., 2002. Monte Carlo modeling of the thermal conductivity of porous cometary ice. Icarus 157, 219–227. doi:10.1006/icar.2002.6815.

Thomas, P.C. et al., 2005. Differentiation of the asteroid Ceres as revealed by its shape. Nature 437, 224226. doi:10.1038/nature03938.

Van Essen, V.M. et al., 2009. Characterization of salt hydrates for compact seasonal thermochemical storage. Proceedings of Energy Sustainability, ES2009-90289.

Waples, D.W., Waples, J.S., 2004. A review and evaluation of specific heat capacities of rocks, minerals, and subsurface fluids. Part 1: Minerals and nonporous rocks. Nat. Resour. Res. 13, 97–122. doi:10.1023/B:NARR.0000032647.41046.e7.

Weidenschilling, S.J., 2008. Accretion of planetary embryos in the inner and outer Solar System. Phys. Scr. T130, 014021.

Wilson, L., Keil, K., Browning, L.B., Krot, A.N., Bourcier, W., 1999. Early aqueous alteration, explosive disruption, and re-processing of asteroids. Meteorit. Planet. Sci. 34, 541–557.

Zent, A.P., Hudson, T.L., Hecht, M.H., Cobos, D., Wood, S.E., 2010. Initial results of the thermal and electrical conductivity probe (TECP) on Phoenix. J. Geophys. Res. 115, E00E14. doi:10.1029/2009JE003420.

Zolotov, M.Y., 2009. On the composition and differentiation of Ceres. Icarus 204, 183–193.